Magnetic Resonance in Solids

Electronic Journal

Harmony in Flux: Coexistence of Superconductivity and Magnetism[†]

F.M. Siraev, M.V. Avdeev, Yu.N. Proshin
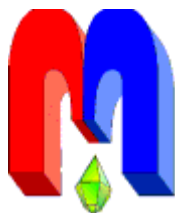
Institute of Physics, Kazan Federal University, Kazan 420008, Russia

E-mail: avdeev.maxim.kfu@gmail.com

This article is a brief overview of our recent work on theoretical studies of the interaction of magnetism and superconductivity in nanostructures. General approaches to the analysis of this interaction are discussed and the unified essence of the problem is revealed: the search for new phenomena and effects in such systems. Various aspects of this problem are considered, including proximity effects, solitary superconductivity, and inhomogeneous superconducting states. Approaches based on the properties of the band structure and Fermi surface for ferromagnets and superconductors in contact are considered in the context of predicting possible effects and explaining observed phenomena. The possibilities of further research in this area are discussed in order to expand our understanding of the physics of magnetic superconductors and develop new technologies based on them.

Introduction

In modern condensed matter physics, the interaction of magnetism and superconductivity is observed, which is an important area of research. This interaction in artificiall heterostructures consisting of superconducting S and ferromagnetic materials F due to the proximity effect and interplay between the S and F parameter orders leads to the emergence of new interesting phenomena and effects that have potential significance for fundamental and applied sciences (see reviews [1–8] and the references therein). Among them, we can note such phenomena as the reentrant [9–11], solitary superconductivity [11, 12], long-range spin-singlet supercurrent in ferromagnet nanowires [13], nonmonotonic behaviors of the critical temperature T_c as function of the mutual alignment of the magnetizations of the F layers [14, 15] and so on. In such nanostructures and low-dimensional systems, this interaction can lead to the emergence of new superconducting states, changes in critical parameters, and the creation of new opportunities for the development of superconducting devices with controlled properties [1, 3, 4, 12, 16–18].

In this context, various aspects of the interaction of magnetism and superconductivity are of interest to researchers. It is especially important to study the effects of proximity between magnetic and superconducting materials, as well as the possibility of the appearance of inhomogeneous superconducting states. It is also important to take into account the influence of the anisotropy of the Fermi surface and the properties of the structure of the ferromagnetic zone on the characteristics of superconductivity in nanostructures. In this brief review, we use the results of our recent studies [9–13, 18–33]

1. Solitary Superconductivity

The main idea behind isolated superconductivity lies in its manifestation within layered heterostructures, where ferromagnetic (F) and superconducting (S) layers coexist. Proximity effect allows superconducting correlations to penetrate into the F-layer, while the magnetic order in the

---

[†]This paper is dedicated to Professor Boris I. Kochelaev on the occasion of his 90th birthday.

F-layer significantly influences superconductivity near the FS interface. Isolated superconductivity, predicted theoretically, emerges in systems like F_1F_2S under the influence of an external magnetic field, forming a localized region on the phase diagram where superconductivity appears with increasing F-layer thickness. Its existence relies on the antiparallel alignment of magnetizations in F-layers, facilitating partial compensation of exchange fields and enabling isolated superconductivity. This phenomenon becomes particularly relevant for potential applications like superconducting spin valves [16–18]. Notably, the behavior of isolated superconductivity is strongly influenced by electron-electron pairing interactions in ferromagnetic metals, especially evident in systems partially or fully compensating magnetization, such as three-layer thin film systems in antiparallel states. The consideration of such interactions has explained unexpectedly high critical temperatures in certain systems, like Gd/La superlattices, underscoring the importance of electron pairing in understanding isolated superconductivity's emergence, even in the presence of strong ferromagnetism.

We consider a three-layer F_1F_2S system in the dirty limit [18–20]. This allows us to use an approach based on the Usadel equations, which also takes into account the interelectronic interaction in both F-layers. The critical temperature of the superconducting transition T_c, taking into account the electron-electron interaction in ferromagnetic layers, is determined from a system of self-consistent equations [34] for superconducting parameters of the order $\Delta_{s,f}(\mathbf{r})$ (where the indices "s", "f" denote S and F layers accordingly):

$$\Delta_s \ln t = 2\pi T_c \mathrm{Re} \sum_{\omega>0}^{\infty} \left[F_s - \frac{\Delta_s}{\omega} \right],$$

$$\Delta_i \left(\ln t + \ln \frac{T_{cs}}{T_{ci}} \right) = 2\pi T_c \mathrm{Re} \sum_{\omega>0}^{\infty} \left[F_{fi} - \frac{\Delta_i}{\omega} \right], \quad i = (f1, f2). \tag{1}$$

Here $t = T_c/T_{cs}$ is the reduced critical temperature, T_{cs} is the critical temperature of the massive S sample, T_{ci} is the "virtual" critical temperature F_i of the layers at zero exchange field $I_i = 0$. Summation in (1) is performed using the Matsubar frequencies ω.

In the dirty limit, the paired amplitude $F_{s,(i)}$ satisfies the Usadel equations [35–37]: for the S-layer:

$$\left[|\omega| - \frac{D_s}{2} \frac{d^2}{dx^2} \right] F_s(x, \omega) = \Delta_s(x) \tag{2}$$

for the F-layer:

$$\left[|\omega| - iI_{fi} - \frac{D_{fi}(I)}{2} \frac{d^2}{dx^2} \right] F_{fi}(x, \omega) = \Delta_{fi}(x),$$

$$D_{fi}(I) = \frac{D_{fi}}{1 - 2iI\tau_f} \tag{3}$$

where $D_{s,fi}$ is the diffusion coefficient in the corresponding layers, τ_f is the scattering time on non-magnetic impurities in the F-layers. Modified Kupriyanov Lukichev boundary conditions [38], obtained microscopically in [10], were used for the paired amplitude. They have the form

$$\frac{4D_{f1}(I)}{\sigma_f v_{\mathrm{F}}^{f1}} \frac{d}{dx} F_{f1} = \frac{4D_{f2}(I)}{\sigma_f v_{\mathrm{F}}^{f2}} \frac{d}{dx} F_{f2} = F_{f2} - F_{f1},$$

$$\frac{4D_s}{\sigma_f v_{\mathrm{F}}^s} \frac{d}{dx} F_s = \frac{4D_{f2}(I)}{\sigma_f v_{\mathrm{F}}^{f2}} \frac{d}{dx} F_{f2} = F_s - F_{f2} \tag{4}$$

for F_1F_2- and F_1S- interfaces and

$$\frac{d}{dx} F_{f1,s} = 0 \tag{5}$$

on the outer borders, respectively. The parameters σ_s and σ_f determine the transparency of the boundary from the S and F layers.To solve Eqs. (2) and (3), we use the approximation $\Delta_{s,f}(x) \approx \Delta_{s,f}(x) = \Delta_{s,f}$. Thus, the solutions of Eqs. (2) and (3) for the F_1F_2S system have the form

$$F_{f1} = \frac{\Delta_1}{\omega - iI_1} + C_1(\omega) \cosh\left(k_{I1}(x + d_{f1} + d_{f2})\right), \; (-d_{f1} - d_{f2} < x < -d_{f2})$$

$$F_{f2} = \frac{\Delta_2}{\omega - iI_2} + A(\omega) \cosh\left(k_{I2}x\right) + B(\omega) \sinh\left(k_{I2}x\right), \; (-d_{f2} < x < 0) \quad (6)$$

$$F_s = \frac{\Delta_s}{\omega} + C_s \cosh\left(k_s(x - d_s)\right), \; (0 < x < d_s)$$

where $k_s^2 = 2\omega/D_s$, $k_I^2 = 2(\omega - iI)/D_f(I)$, and the coefficients $C1$, A, B, and C_s are fixed by boundary conditions (4) and (5) and are expressed in terms of linear combinations of the order parameters Δ_s, $\Delta 1$, and Δ_2. Then, substituting Eqs. (6) into Eq. (1) and solving the resulting secular equation, we determine the critical temperature T_c for the F_1F_2S system.

Figure 1a shows the calculated reduced critical temperature t as a function of the thickness d_{f2} of the intermediate layer F_2 at various values of the ratio T_{cs}/T_{cf} and the fixed thickness of the outer layer F_1 $d_{f1} = 2\xi_{I1}$ (here and below, all lengths referring to the S and F layers are presented in units of ξ_S and ξ_I, respectively). As was mentioned above, such an extraordinary nonmonotonic dependence $T_c(d_{f2})$ is called soliftary superconductivity.
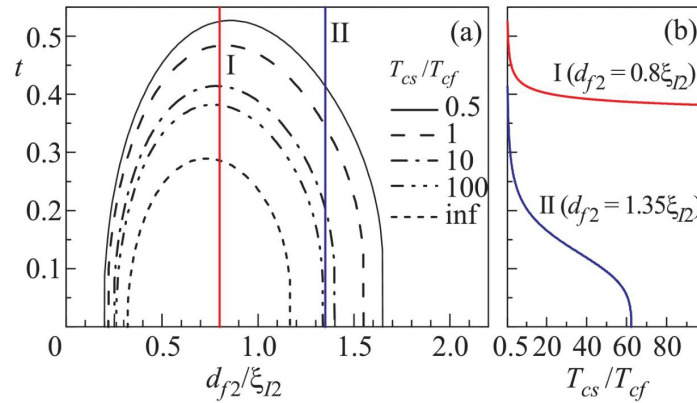
Figure 1. (Color online) Phase diagram of the F_1F_2S system in the antiparallel state. (a) Reduced critical temperature t versus the reduced thickness d_{f2}/ξ_I of the layer at various values of the parameter T_{cs}/T_{cf}. The thickness of the outer layer F_1 is fixed: $d_{f2} = 2\xi_I$. (b) Reduced critical temperature t versus ratio T_{cs}/T_{cf} at two different thicknesses of the F_2 layer (sections I and II in panel (a)). The other parameters are $d_s/\xi_S = 1.1$, $\ell_s/\xi_S = 0.7$, $\sigma_s = 100$, $\sigma_f = 100$, $\ell_{f1}/\xi_{I1} = \ell_{f2}/\xi_{I2} = 0.3$, and $I_1/\pi T_{cs} = I_2/\pi T_{cs} = 6$. (This figure is taken from paper [18])

The critical temperature T_c in the solitary superconductivity regime significantly depends on the ratio T_{cs}/T_{cf} (see Fig. 1a). In particular, for $T_{cs}/T_{cf} = 0.5$, the critical temperature is $t \approx 0.5$ at $d_{f2} = 0.8\xi_I$ (vertical straight line I in Fig. 1a), which is almost twice as high as the t value in the absence of the electron–electron interaction ($t \approx 0.25$, the point of intersection of the lower dashed line and vertical straight line I in Fig. 1a). The region of solitary superconductivity is narrowed with an increase in T_{cs}/T_{cf}. However, the position of the maximum t ($d_{f2} \approx 0.8\xi_I$) hardly depends on the parameter T_{cs}/T_{cf}.

Figure 1b shows the dependence of t on the ratio T_{cs}/T_{cf} at two fixed values of the thickness of the layer F_2. The largest change in the critical temperature is observed in the region $T_{cs} \sim T_{cf}$.

States with solitary superconductivity can be controlled by changing the mutual orientation of the magnetizations, are interesting and promising for the possible implementation of a spin valve [39]. The magnetization of the outer layer F_1 is pinned by an additional layer of antiferromagnetic dielectric, while the orientation of the magnetization of the intermediate layer F_2 can be changed by an external magnetic field. Thus, when the magnetic field in the system changes, the spin valve switches from a superconducting to a resistive state-back and forth. In this regard, we emphasize that one of the important characteristics of the spin valve is the difference $\Delta T_c = T_c^{\mathrm{AP}} - T_c^{\mathrm{P}}$ between critical temperatures in the AR and P states. The higher the value of the ΔT_c, the more stable its operation will be. Note once again that the difference ΔT_c, in the mode of isolated superconductivity, coincides with the critical temperature, $\Delta T_c = T_c^{\mathrm{AP}}$, since in this case $T_c^{\mathrm{P}} = 0$. The experimental detection of states with solitary superconductivity in F_1F_2S systems looks quite realistic and feasible.

2. Long-range spin-singlet proximity effect

Recent advances in the fabrication and design of layered superconductor (S-) ferromagnet (-F) structures, driven by the proximity effect, have significantly advanced superconducting spintronics. A key area of discussion has been the origin of the long-range proximity effect, where singlet superconducting correlations penetrate deeply into the ferromagnetic (F) region, despite the exchange field's tendency to align electron spins in parallel, disrupting antiparallel superconducting Cooper pairs. The penetration depth (LSF) in conventional ferromagnets like Co and Fe is estimated to be around 1-10 nm, much smaller than the corresponding length in nonferromagnetic (N) metals, which can reach 0.1–$1\,\mu$m at low temperatures. Additionally, the Fulde-Ferrell-Larkin-Ovchinnikov (FFLO) superconducting state in ferromagnets exhibits oscillatory behavior, unlike normal metals. The long-range proximity effect occurs when superconducting correlations become insensitive to the exchange field, with LSF comparable to the coherence length in the normal state (LSN), particularly feasible for superconducting triplet correlations. Triplet superconductivity arises in SF multilayers with non-collinear magnetizations or in the presence of domain walls or spin-active interfaces. Recent experiments by Wang et al. observed a long-range singlet proximity effect in clean SFS structures, demonstrating zero resistance and significant critical current magnitudes in cobalt nanowires. Following this, Konschelle et al. proposed an explanation based on one-dimensional (1D) Eilenberger equations, suggesting that the standard singlet proximity effect becomes long-ranged if the ferromagnet is treated as a 1D ferromagnetic wire in the ballistic transport regime. Another model linked long-range triplet superconducting correlations with spin-orbit interactions in F nanowires, where the effective exchange field depends on quasiparticle momentum, affecting the phase gain along trajectories.

Our approach is based on the known physical fact that the effective masses of the conduction electrons for spin bands $(1/m_\alpha)_{ij} = \partial^2 \epsilon_\alpha(\mathbf{k})/\partial k_i \partial k_j$ are generally different in real ferromagnets [13]. Here $\alpha = \uparrow (\downarrow)$ labels spins in the majority (minority) spin subband, respectively. Indeed, this feature can lead to a compensation of the total momentum of the Cooper pair in a ferromagnet. It is easy to understand within the simple picture of the FFLO pairing mechanism with total momentum $\mathbf{q}$ of the pair (where q is much less than the Fermi momentum k_F). In a ferromagnet, the momentum $\mathbf{q}$ is obtained from the condition $(\mathbf{k}_F + \mathbf{q}/2)^2/2m_\uparrow - h = (-\mathbf{k}_F + \mathbf{q}/2)^2/2m_\downarrow + h$. It follows immediately that $\mathbf{q}\mathbf{k}_F/2M \approx h - \eta k_F^2/2M$, where $M = 2m_\uparrow m_\downarrow/(m_\downarrow + m_\uparrow)$ and the mismatch parameter $\eta = (m_\downarrow - m_\uparrow)/(m_\downarrow + m_\uparrow)$. Thus, the total momentum of the FFLO-like pair completely vanishes at $\eta \approx h/E_F \approx 1$, where E_F is the Fermi energy. It leads to a long-range spatial extent of the induced superconductivity in a

ferromagnetic nanowire.

3. BCS and FFLO States in Magnetic Superconductors

In this part, we discuss the possibility of the existence and competition between the FFLO and BCS phases in the background of a cryptoferrromagnetic state in pure single-crystalline samples. Recent studies have shown that the peculiarities of the zone structure of a ferromagnet can significantly modify the spatial scale of the order parameter modulation induced in the ferromagnet due to the proximity effect. Based on these results, we consider the effects related to the fact that the majority and minority spin subbands, split by the exchange field, can approach or touch each other on the Fermi surface in certain crystallographic directions. Such a mechanism is possible if the effective masses of the majority and minority spin subbands differ, such that the condition $m_\downarrow > m_\uparrow$ is fulfilled. For clarity, let's consider the simple case of parabolic zones, where the total momentum of the pair in the FFLO state can be estimated from the condition

$$(\mathbf{k}_0 + \mathbf{q}/2)^2/2m_\uparrow - h = (-\mathbf{k}_0 + \mathbf{q}/2)^2/2m_\downarrow + h$$

. Considering that $k_0 \approx k_F$, this can be represented as $\mathbf{k}_0\mathbf{q}/2M = h - \eta\mathbf{k}_0^2/2M$, where $\eta = (m_\downarrow - m_\uparrow)/(m_\downarrow + m_\uparrow)$, $M = 2m_\uparrow m_\downarrow/(m_\uparrow + m_\downarrow)$. In the limiting case when the effective masses coincide ($\eta = 0$), we obtain the well-known result. Thus, in homogeneous samples, the proximity of the values of η and h/E_F can lead to a significant weakening of the influence of the exchange field on superconductivity. However, the estimates given are valid for the case of homogeneous magnetization. In the case of a cryptoferrromagnetic state, the magnetic order is modulated in space and in the simplest case represents a helicoidal magnetic structure with a spatial period. A similar problem was previously considered in the context of the problem of coexistence of superconductivity and magnetism in the compound $ErRh_4B_4$. However, the previously considered case of superconducting state was associated only with spatially homogeneous order parameter. Later, non-homogeneous states like FFLO were considered against the background of antiferromagnetic ordering [40].

Here we consider the more general D-dimensional case, where the superconducting order parameter is modulated in space with a wave vector $\mathbf{q}$, the magnitude and direction of which are determined by the maximization condition of the critical temperature T_c. Accordingly, we seek solutions in the form of $\Delta(\mathbf{r}) = \Delta_\mathbf{q} e^{i\mathbf{q}\mathbf{r}}$. Thus, the superconducting part of the Hamiltonian takes the form

$$\hat{H}_{SC} = \sum_\mathbf{k} \Delta_\mathbf{q} \psi^\dagger_{\mathbf{k}+\mathbf{q}/2\uparrow} \psi^\dagger_{-\mathbf{k}+\mathbf{q}/2\downarrow} + \text{h.c.} \tag{7}$$

Meanwhile, the Hamiltonian in the case of non-homogeneous magnetization and taking into account the differences in effective masses ($\eta = 0$) is written as

$$\hat{H}_0 = -\frac{1}{2M}\nabla^2 - E_F - \mathbf{h}\hat{\boldsymbol{\sigma}} + \frac{\eta}{2M}\frac{1}{2}\left[\mathbf{e}_h\hat{\boldsymbol{\sigma}}\nabla^2 + \nabla^2\mathbf{e}_h\hat{\boldsymbol{\sigma}}\right], \tag{8}$$

where we have introduced the unit vector along the direction of the exchange field $\mathbf{e}_h = \mathbf{h}/h$. It is also worth noting that the last term is written in a symmetric form, ensuring the Hermiticity of this operator. Next, it is convenient to perform a unitary transformation $\hat{H}_0 \to \hat{U}\hat{H}_0\hat{U}^\dagger$, where $\hat{U}(\mathbf{r}) = \exp(iQx\hat{\sigma}_x/2)$, which diagonalizes the term $\mathbf{h}\hat{\boldsymbol{\sigma}}$ (note that $\hat{H}_{SC}$ is invariant under this transformation). Transitioning to the momentum representation, we obtain the effective Hamiltonian of free electrons

$$\hat{H}_{\text{eff}} \approx \xi + \frac{1}{2}\boldsymbol{v}_0\mathbf{q} - h_{\text{eff}}\,\hat{\sigma}_z - \frac{1}{2}\mathbf{Q}\,\boldsymbol{v}_0\hat{\sigma}_x, \tag{9}$$

where $\xi = k^2/2M - E_F$, $\boldsymbol{v}_0 = \mathbf{k}_0/M$, $k_0 = \sqrt{2ME_F}$, and it is assumed that $k_0 \gg Q, q$. This system is described by Gor'kov equations, which in matrix form can be represented as

$$\begin{pmatrix} \hat{G}_+^{-1} & i\hat{\sigma}_y\Delta_{\mathbf{q}} \\ i\hat{\sigma}_y\Delta_{\mathbf{q}}^* & \hat{G}_-^{-1} \end{pmatrix} G(\xi, \mathbf{q}, \omega) = \hat{1}, \tag{10}$$

where $\hat{G}_\pm^{-1} = \pm i\omega - \hat{H}_{\text{eff}}(\pm\mathbf{q}, \pm\mathbf{Q})$ (here $\omega = \pi T(2n+1)$ is the Matsubara frequency). Accordingly, the self-consistency equation for the order parameter takes the form

$$\Delta_{\mathbf{q}} = \frac{\lambda}{2}\pi T \sum_\omega \text{Re}\langle \text{Tr}\,\hat{G}(\mathbf{q}, \omega)\hat{\gamma} \rangle_{\mathbf{n}}, \tag{11}$$

where

$$\hat{G}(\mathbf{q}, \omega) = \int \frac{d\xi}{2\pi} \hat{G}(\xi, \mathbf{q}, \omega), \quad \hat{\gamma} = \begin{pmatrix} 0 & -i\hat{\sigma}_y \\ -i\hat{\sigma}_y & 0 \end{pmatrix}, \tag{12}$$

and the angle brackets $\langle ... \rangle$ signifies averaging over the direction of momentum, and summation is cut off at the Debye frequency. Near the transition temperature T_c, when the order parameter is small, the right-hand side of equation (11) can be expanded to first order in $\Delta_{\mathbf{q}}$. Thus, the self-consistency equation is reduced to a simpler form

$$\ln \frac{T_c}{T_{c0}} = \pi T_c \sum_\omega \left\langle \frac{1}{\Omega} - \frac{1}{|\omega|} - \frac{h_{\text{eff}}^2}{\Omega(\Omega^2 + \Gamma^2)} \right\rangle_{\mathbf{n}}, \tag{13}$$

where $\Omega = |\omega| + i\mathbf{q}\boldsymbol{v}_0/2$, $\Gamma^2 = h_{\text{eff}}^2 + (\mathbf{Q}\boldsymbol{v}_0/2)^2$, and T_{c0} is the critical temperature of the homogeneous superconducting state at $h_{\text{eff}} = 0$. Numerical solutions of equation (13) are presented in Fig. 2. The upper panels of Fig. 2(a)-(c) show the dependence of the reduced critical temperature $t = T_c/T_{c0}$ on the magnitude of the magnetic structure vector $Q\xi_{s0}$ (here $\xi_{s0} = v_0/2\pi T_{c0}$ is the coherence length) and the effective exchange field $h_{\text{eff}}/\pi T_{c0}$. For comparison, case (a) corresponds to homogeneous superconducting state when $\mathbf{q} = 0$ (this particular case was considered in the work [36]). The light dashed line indicates the boundary between the normal (NS) and homogeneous superconducting (BCS) phases. Here, the competition of two factors is clearly visible: on the one hand, as mentioned above, the exchange field tends to suppress superconductivity, and on the other hand, the increase in $\mathbf{Q}$ leads to the opposite effect. Physically, this can be easily understood from the following reasoning: with the increase in the wave vector $\mathbf{Q}$, the spatial period of the magnetic structure $L = 2\pi/Q$ decreases, and when it becomes comparable to the coherence length ξ_{s0}, the Cooper pair "senses" some averaged value of the exchange field, which turns out to be significantly smaller than in the case of homogeneous magnetization, leading to an increase in the critical temperature.

However, a much more interesting picture emerges when considering the possibility of the emergence of a non-uniform superconducting state of the FFLO type with a spatial modulation wave vector $\mathbf{q}$. Indeed, due to the anisotropy induced by the distinguished direction in space, defined by the magnetic structure vector $\mathbf{Q}$, the critical temperature in the FFLO phase acquires an angular dependence $T_c(\cos\psi)$, where ψ is the angle between the vectors $\mathbf{q}$ and $\mathbf{Q}$. Thus, in Fig. 2(b, c), phase diagrams are given for two limiting cases, when the order parameter is modulated in space parallel to the magnetic structure vector ($\mathbf{q} \parallel \mathbf{Q}$ in Fig. 2(b)) and perpendicular to it ($\mathbf{q} \perp \mathbf{Q}$ in Fig. 2(c)). In both phase diagrams, the presence of a localized FFLO phase is clearly visible (the boundary between different phases is indicated by a light dashed line), and its area is significantly larger when the vectors $\mathbf{q}$ and $\mathbf{Q}$ are oriented perpendicular
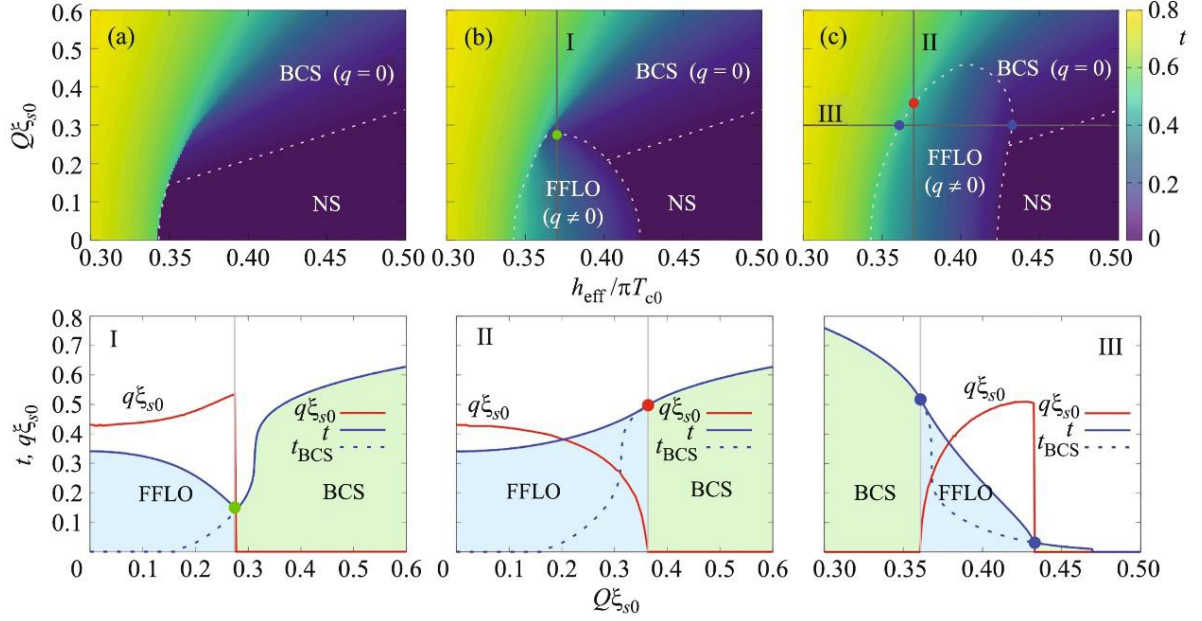
Figure 2. (Color online) Phase diagrams of states. (a–c) Color maps of the reduced critical temperature t on the $(Q\xi_{s0}, h_{\text{eff}}/\pi T_{c0})$ plane for (a) the homogeneous case ($q = 0$), (b) $\mathbf{q} \parallel \mathbf{Q}$, and (c) $\mathbf{q} \perp \mathbf{Q}$. The lower panels show the respective sections I-III marked in panels (b) and (c). (This figure is taken from paper [12])

($\psi = \pi/2$), and, accordingly, such a configuration, being energetically favorable, has a higher critical temperature.

The competition between the BCS and FFLO states in the presence of helical magnetic ordering reveals a tri-critical point at the boundary separating these two phases. This implies that the type of phase transition from the BCS state to the FFLO state and vice versa depends on the path on the phase diagram along which this transition occurs. On the lower panel of Fig. 2, slices corresponding to lines I-III on the phase diagrams (see Fig. 2(b) and (c)) are presented. These slices also show the behavior of the wave vector $\mathbf{q}$ (solid red line). Crossing the FFLO-BCS boundary along line I, the wave vector $\mathbf{q}$ undergoes a sudden change in its value, indicating a first-order phase transition. Conversely, moving along line II in Fig. 2(c), there is a continuous monotonic change in the magnitude of $\mathbf{q}$ from its initial value $q\xi_{s0} \approx 0.45$ in the FFLO phase to zero at the FFLO-BCS boundary, corresponding to a second-order phase transition. Moving along line III, starting from the BCS phase (where $q = 0$), crossing the BCS-FFLO boundary, the wave vector monotonically increases from zero to a value of $q\xi_{s0} \approx 0.5$ at the opposite FFLO-BCS boundary, after which it suddenly drops to zero. Here, we observe two transitions: first, a second-order phase transition, followed by a first-order transition. For the second-order transition, the critical temperature monotonically increases with increasing $\mathbf{Q}$, while for the first-order transition, there is a characteristic kink at the boundary between the FFLO and BCS states. These findings underscore the complex interplay between different types of phase transitions and the dependence on the specific path traversed on the phase diagram.

4. Results and discussion

The intricate interplay between superconductivity and magnetism, as revealed by modern research, unveils fascinating aspects of these fundamental phenomena. Exploring the nuances of their coexistence not only enriches our understanding of microscopic physical processes but also

holds promise for practical applications across various domains, including energy and information technologies. These studies offer insights into the quantum realm, opening up new horizons in material physics. Deepening our understanding of the interplay between superconductivity and magnetism paves the way for advancements in science and technology, shaping the future of innovation.

Acknowledgments

References

1. Izyumov Y. A., Proshin Y. N., Khusainov M. G., *Physics-Uspekhi* **45**, 109 (2002)

2. Golubov A. A., Kupriyanov M. Y., Il'Ichev E., *Reviews of Modern Physics.* **76**, 411 (2004)

3. Buzdin A. I., *Reviews of Modern Physics.* **77**, 935 (2005)

4. Bergeret F. S., Volkov A. F., Efetov K. B., *Reviews of Modern Physics.* **77**, 1321 (2005)

5. Efetov K. B., Garifullin I. A., Volkov A. F., Westerholt K., in *Magnetic Heterostructures: Advances and Perspectives in Spinstructures and Spintransport* (Springer, 2008) pp. 251–290

6. Eschrig M., *Reports on Progress in Physics* **78**, 104501 (2015)

7. Doukas D. I., *IEEE Transactions on Applied Superconductivity* **29**, 1 (2019)

8. Mel'nikov A., Mironov S. V., Samokhvalov A. V., Buzdin A. I., *Physics-Uspekhi* **192**, 1339 (2022)

9. Khusainov M. G., Proshin Y. N., *Physical Review B* **56**, R14283 (1997)

10. Proshin Y. N., Khusainov M. G., *Journal of Experimental and Theoretical Physics* **86**, 930 (1998)

11. Proshin Y. N., Avdeev M. V., *Journal of Low Temperature Physics* **179**, 113 (2015)

12. Siraev F. M., Kutuzov A. S., Avdeev M. V., Proshin Y. N., *Journal of Experimental and Theoretical Physics Letters* **111**, 139 (2020)

13. Avdeev M. V., Proshin Y. N., *Physical Review B* **97**, 100502 (2018)

14. Fominov Y. V., Golubov A. A., Kupriyanov M. Y., *Journal of Experimental and Theoretical Physics Letters* **77**, 510 (2003)

15. Fominov Y. V., Golubov A. A., Karminskaya T. Y., Kupriyanov M. Y., Deminov R. G., Tagirov L. R., *Journal of Experimental and Theoretical Physics Letters* **91**, 308 (2010)

16. Leksin P. V., Garif'yanov N. N., Kamashev A. A., Fominov Y. V., Schumann J., Hess C., Kataev V., Büchner B., Garifullin I. A., *Physical Review B* **91**, 214508 (2015)

17. Singh A., Voltan S., Lahabi K., Aarts J., *Physical Review X* **5**, 021019 (2015)

18. Avdeev M. V., Proshin Y. N., *Journal of Magnetism and Magnetic Materials* **440**, 116 (2017)

19. Avdeev M. V., Proshin Y. N., *Journal of Low Temperature Physics* **185**, 453 (2016)

20. Avdeev M. V., Proshin Y. N., *Journal of Experimental and Theoretical Physics Letters* **102**, 96 (2015)

21. Proshin Y. N., Avdeev M. V., *Journal of Magnetism and Magnetic Materials* **383**, 166 (2015)

22. Proshin Y. N., Khusainov M. M., Minnullin A., *Physica status solidi (c)* **11**, 1080 (2014)

23. Avdeev M. V., Proshin Y. N., *Superconductor Science and Technology* **27**, 035006 (2014)

24. Avdeev M. V., Proshin Y. N., *Journal of Experimental and Theoretical Physics* **117**, 1101 (2013)

25. Proshin Y. N., Avdeev M. V., Khusainov M. M., Khusainov M., *Journal of magnetism and magnetic materials* **324**, 3478 (2012)

26. Avdeev M. V., Khusainov M., Proshin Y. N., Tsarevskii S., *Superconductor Science and Technology* **23**, 105005 (2010)

27. Khusainov M. G., Khusainov M. M., Ivanov N. M., Proshin Y. N., *Journal of Experimental and Theoretical Physics Letters* **90**, 359 (2009)

28. Khusainov M. G., Khusainov M. M., Ivanov N. M., Proshin Y. N., *Journal of Experimental and Theoretical Physics Letters* **90**, 124 (2009)

29. Izyumov Y. A., Khusainov M. G., Proshin Y. N., *Low Temperature Physics* **32**, 809 (2006)

30. Proshin Y. N., Zimin A., Fazleev N. G., Khusainov M. G., *Physical Review B* **73**, 184514 (2006)

31. Khusainov M. G., Khusainov M. M., Proshin Y. N., *Journal of Magnetism and Magnetic Materials* **300**, e243 (2006)

32. Khusainov M. G., Proshin Y. N., *Physics-Uspekhi* **173**, 1385 (2003)

33. Proshin Y. N., Khusainov M. G., *Journal of Experimental and Theoretical Physics Letters* **66**, 562 (1997)

34. Abrikosov A., Gorkov L., *Sov. Phys. Journal of Experimental and Theoretical Physics* **12**, 1243 (1961)

35. Usadel K., *Physical Review Letters* **25**, 507 (1970)

36. Radović Z., Dobrosavljević-Grujić L., Buzdin A., Clem J., *Physical Review B* **38**, 2388 (1988)

37. Krunavakarn B., Yoksan S., *Physica C: Superconductivity* **440**, 25 (2006)

38. Kupriyanov M. Y., Lukichev K., *Journal of Experimental and Theoretical Physics* **94**, 139 (1988)

39. Oh S., Youm D., Beasley M., *Applied physics letters* **71**, 2376 (1997)

40. Buzdin A., Bulaevskiĭ L., Kulich M., Panyukov S., *Physics-Uspekhi* **27**, 927 (1984)